Title: Role of ferroptosis in cisplatin-induced acute nephrotoxicity in mice

Short title: Role of ferroptosis in cisplatin-induced nephrotoxicity

Yasumasa Ikeda[a], Hirofumi Hamano[b], Yuya Horinouchi[a], Licht Miyamoto[c], Tasuku Hirayama[d], Hideko Nagasawa[d], Toshiaki Tamaki[a,e], Koichiro Tsuchiya[c]

[a]Department of Pharmacology, [c]Department of Medical Pharmacology, Institute of Biomedical Sciences, Tokushima University Graduate School, Tokushima, Japan

[b]Department of Pharmacy, Tokushima University Hospital, Tokushima, Japan

[d]Laboratory of Pharmaceutical and Medicinal Chemistry, Gifu Pharmaceutical University, Gifu, Japan

[e]Anan-Medical Center, Anan, Japan

Corresponding author: Yasumasa Ikeda, MD, PhD Department of Pharmacology, Institute of Biomedical Sciences, Tokushima University Graduate School, 3-18-15 Kuramoto-cho, Tokushima 770-8503, Japan

E-mail: yasuike@tokushima-u.ac.jp   Tel: +81-88-633-7061, Fax: +81-88-633-7062

1

Abstract

Background: Cisplatin is widely used as an antitumor drug for the treatment of solid tumors. However, its use has been limited owing to nephrotoxicity, a major side effect. The mechanism of cisplatin-induced nephrotoxicity (CIN) has long been investigated in order to develop preventive/therapeutic drugs. Ferroptosis is a newly identified form of non-apoptotic regulated cell death induced by iron-mediated lipid peroxidation and is involved in the pathophysiology of various diseases. In this study, we examined the role of ferroptosis in CIN.

Methods: We evaluated the role of ferroptosis in CIN by in vivo experiments in a mouse model.

Results: Cisplatin increased the protein expressions of transferrin receptor-1 and ferritin, and iron content in the kidney of mice. In addition, treatment with cisplatin augmented renal ferrous iron and hydroxyl radical levels with co-localization. Mice administered cisplatin demonstrated kidney injury, with renal dysfunction and increased inflammatory cytokine expression; these changes were ameliorated by Ferrostatin-1 (Fer-1), an inhibitor of ferroptosis. The expression of the ferroptosis markers, COX2 and 4-

hydroxynonenal (4-HNE), increased with cisplatin administration, and decreased with the administration of Fer-1. By contrast, cisplatin-induced apoptosis and necroptosis were inhibited by treatment with Fer-1. Moreover, deferoxamine, an iron chelator, also inhibited CIN, with a decrease in the expression of COX-2 and 4-HNE. Conclusion: Ferroptosis is involved in the pathogenesis of CIN and might be used as a new preventive target for CIN.

Introduction

Cisplatin is globally used for the treatment of human malignancies. Despite its efficacy, cisplatin use is associated with severe side effects, such as bone marrow suppression, peripheral neuropathy, ototoxicity, anaphylaxis, and nephrotoxicity (cisplatin-induced nephrotoxicity; CIN). CIN is reported in about 25% of patients on cisplatin chemotherapy [1]. CIN manifests mainly as renal proximal tubule damage due to cellular uptake of cisplatin [2]. The molecular mechanisms underlying CIN include, inflammation, apoptosis, oxidative stress, DNA damage, and mitochondrial dysfunction [3]. Currently, no drugs are available for clinical prevention of CIN, and only hydration therapy with the administration of diuretics, such as furosemide, is used as a preventive measure [4].

Ferroptosis is a new type of programmed cell death mediated through iron-dependent lipid peroxidation [5]. Ferroptosis is mainly induced and promoted by lipid peroxidation due to glutathione (GSH) depletion, decreased activity of GSH peroxidase 4 (GPX4), and the ferrous iron-catalyzing Fenton reaction [6]. Ferroptosis has been reported in various cancers, including liver, colorectal, and breast cancers, and the induction of ferroptosis has been shown to potentiate cancer treatment [7]. Ferroptosis is

also involved in the pathophysiology of neurodegenerative disorders [8,9], stroke [9], acute kidney injury (AKI) [9], and cardiac injury [10]. Inhibition of ferroptosis ameliorates conditions such as Huntington's disease [8], brain hemorrhage [9], AKI [11], and cardiac ischemia/reperfusion injury [10]. Thus, the modulation of ferroptosis might help develop preventive and therapeutic targets.

In a previous study, cisplatin administration increased the bleomycin-detectable iron content and hydroxyl radical formation in rat renal tubular cells. Furthermore, iron chelator treatment was found to alleviate marked kidney dysfunction and histological injury in cisplatin-induced AKI in rats [12]. Iron might play a critical role in mediating cisplatin-induced kidney injury; however, the association between CIN and ferroptosis remains unclear.

In this study, we found that cisplatin induced an increase in renal iron content and that this effect could be prevented by a ferroptosis inhibitor.

Materials and Methods

Cisplatin (Landa™), Ferrostatin-1 (Fer-1), and deferoxamine (DFO) were purchased from Nippon Kayaku Co. Ltd. (Tokyo, Japan), FUJIFILM Wako Pure Chemical Corporation (Osaka, Japan), and Cayman Chemical (Ann Arbor, MI), respectively.

Hydroxyphenyl fluorescein (HPF) was purchased from Goryo Chemical (Sapporo, Japan). The following commercially available antibodies were used: anti-4-hydroxynonenal (4-HNE; MHN-100P, Japan Institute for the Control of Aging, Nikken SEIL Co., Ltd., Shizuoka, Japan), anti-cleaved Caspase-3 (Asp175) (9661) (Cell Signaling Technology, Danvers, MA), anti-cyclooxygenase (COX)-2 (160126) (Cayman Chemical, Ann Arbor, MI), anti-glutathione peroxidase (GPX)-4 (14432-1-AP)(Proteintech, Rosemont, IL), anti-transferrin receptor 1 (TfR) (13–6800) (Life Technologies, Carlsbad, CA), anti-ferritin heavy chain (FTH) (sc-25617), and anti-ß-actin (sc-47778) (Santa Cruz Biotechnology, Inc., Dallas, TX).

CIN mouse models

Seven- to eight-week-old male C57BL/6J mice (22-25 g) were purchased from Nippon CLEA (Tokyo, Japan). The mice were randomly divided into the following groups: vehicle-injected group, cisplatin-injected group, cisplatin + Fer-1-injected group, and cisplatin + DFO-injected group. Mice were treated with intraperitoneal injections of cisplatin (20 mg/kg) or a vehicle. Fer-1 (5 mg/kg), DFO (100 mg/kg), or the vehicle were administered 1 d before, 1 h before, and 1 d after cisplatin injection (a total of three times), respectively. Forty-eight hours after cisplatin injection, the mice were sacrificed, and their

blood and tissue samples were collected and used for analysis. The experimental protocol and drug dose were determined based on those used in previous studies[10,13,14].

In situ detection of labile ferrous iron and hydroxyl radicals

Labile ferrous iron and hydroxyl radicals were detected using FerroOrange (RhoNox-4) [15] and HPF, respectively. In summary, the frozen sections were fixed in 10% neutral formaldehyde for 1 min, washed with Hank's Balanced Salt Solution, and incubated with 1 µM FerroOrange or 5 µM HPF in a dark, humidified container at room temperature for 30 min. After washing, the sections were observed using a fluorescence microscope [16].

Quantification of iron content

The iron content of tissues or cells was measured using an iron assay kit according to the manufacturer's instructions (Metallo Assay LS, Metallogenics, Chiba, Japan) as previously described [16]. The iron concentration was evaluated using tissue weight or protein concentration and expressed as µg of Fe per g of protein concentration.

RNA extraction and mRNA expression

The methods used for RNA extraction, cDNA synthesis, and quantitative RT-PCR have been previously described [17]. The primer sets used in this study are listed in Table 1.

Protein extraction and western blot analysis

Protein preparation and western blotting were performed as previously described [17]. The detected immunoreactive bands were quantified via densitometric analysis using the Image J (version 1.38) software (National Institutes of Health, Bethesda, MD, USA).

Measurement of plasma creatinine and blood urea nitrogen levels

Plasma creatinine and blood urea nitrogen (BUN) levels were measured using an enzymatic method or the urease-GLDH method, respectively (Oriental Yeast Co., Ltd., Shiga, Japan).

Histological analysis

The method used for the histological evaluation of renal tubular damage has been previously described [13]. Hematoxylin and eosin (HE)-stained sections were used for scoring tubular injury (tubular necrosis, brush-border loss, cast formation, tubule

dilatation, and tubular degeneration) as follows: **0,** normal; **1,** < 25%; **2,** 25–50%; **3,** 50–75%, and **4,** > 75%.

TdT-mediated dUTP nick end labeling (TUNEL) staining

Apoptosis in the kidneys was evaluated using TUNEL staining (Apoptosis *in situ* Detection Kit Wako, FUJIFILM Wako Pure Chemical Corporation, Osaka, Japan), followed by counterstaining with methyl green. Semi-quantification of TUNEL-positive cells was performed in ten random fields [13].

Immunohistochemistry

Paraformaldehyde-fixed paraffin-embedded sections were used for the detection of 4-HNE, as previously described [17]. Sections incubated without the primary antibody were used as the negative controls.

Results

Effects of cisplatin on renal iron levels and the induction oxidative stress

First, we examined whether cisplatin altered renal iron levels and induced oxidative stress in mice. Cisplatin increased the production of ferrous iron and hydroxyl radical, and they were colocalized in the kidney, suggesting the occurrence of the Fenton

reaction (Figure 1A-C). Total iron content and TfR and FTH protein expression were increased in the kidney after cisplatin treatment (Figure 1D-F).

Effects of cisplatin on ferroptosis in the kidney

We investigated the effects of cisplatin on ferroptosis in cisplatin-treated mice. Increase in COX-2 levels is a suitable marker for ferroptosis, although COX-2 does not regulate ferroptosis [18]. COX-2 mRNA and protein levels increased in the kidneys of mice treated with cisplatin and decreased following treatment with Fer-1 (Figure 2A). Cisplatin treatment induced a decrease in the levels of GPX4 mRNA; however, treatment with Fer-1 did not cause significant changes in GPX4 mRNA levels. No significant difference in protein levels was observed between the 3 groups (Figure 2B). Cisplatin increased 4-HNE protein levels; 4-HNE is a lipid peroxidation marker in the kidney, and its levels were normalized by treatment with Fer-1 (Figure 2C and D).

Preventive action of Fer-1 against cisplatin-induced kidney injury in mouse models

We evaluated the preventive effects of Fer-1 against CIN. Mice treated with cisplatin showed a significant reduction in body weight but no change in kidney weight (Table 2). Histological analysis showed that cisplatin administration induced kidney injury in mice, but this injury was alleviated by concomitant treatment with Fer-1 (Figure

3A). Except in mice co-treated with Fer-1, the plasma BUN and creatinine levels and the

LCN-2 mRNA level were elevated in the kidneys of all cisplatin-treated mice (Table 2

and Figure 3B). Cisplatin-induced upregulation of inflammatory cytokine mRNAs, such

as those of TNF-α, MCP-1, and IL-6, was also inhibited by treatment with Fer-1 (Figure

3C).

Effects of Fer-1 on apoptosis and necroptosis in CIN

Apoptosis and necroptosis are known to be involved in CIN [3]. We evaluated

the effects of Fer-1 on apoptosis and necroptosis in CIN. Cisplatin increased TUNEL-

positive cell count and cleaved caspase-3 levels (markers of apoptosis) in the kidneys, but

these changes decreased with Fer-1 administration (Figure 4A and B). Moreover,

cisplatin-induced RIPK3 and MLKL mRNA expression (markers of necroptosis) was

suppressed by treatment with Fer-1 (Figure 4C).

Suppressive effects of iron chelation on cisplatin-induced kidney injury

Finally, we evaluated the preventive effects of DFO against CIN via ferroptosis.

Similar to Fer-1, treatment with DFO inhibited the cisplatin-induced upregulation of

COX-2 mRNA(data not shown) and protein expression (Figure 5A). Histological analysis

showed that DFO alleviated cisplatin-induced kidney injury (Figure 5B). Cisplatin-

induced renal dysfunction (reflected by BUN and creatinine levels) and increase in kidney

injury marker level (LCN-2 mRNA) was inhibited by treatment with DFO (Table 3 and

Figure 5C). DFO also reduced cisplatin-induced upregulation of TNF-α, MCP-1, and IL-

6 mRNA levels (Figure 5D). As expected, the preventive action of DFO against CIN may

be partly mediated by the inhibition of ferroptosis.

Discussion

We found that ferroptosis was involved in the pathophysiology of CIN.

Treatment with cisplatin augmented renal iron content and TfR expression. Moreover,

ferrous iron levels were increased in mice treated with cisplatin, and CIN was inhibited

by a ferroptosis inhibitor. Thus, our results indicate the inhibition of ferroptosis as a

potential therapeutic target for the prevention of CIN.

Many previous studies have shown that the occurrence of CIN is mediated

through various mechanisms, including inflammation, apoptosis, and oxidative stress,

and that the inhibition of these mechanisms can alleviate CIN [3,19,20]. In this study,

acute cisplatin treatment induced kidney injury, with increase in inflammation, apoptosis,

and oxidative stress; Fer-1, an inhibitor of lipid peroxidation, suppressed CIN, with a

decrease in inflammation and apoptosis. Necroptosis is also involved in CIN [21], and

cisplatin-induced RIPK3 and MLKL mRNA expression was suppressed by Fer-1. In a previous study, Fer-1 inhibited folic acid-induced kidney injury with a reduction in necroptosis, and zVAD (a necroptosis inhibitor) did not abrogate this effect [22]. The finding indicates that lipid peroxidation is an upstream process of necroptosis in CIN. Therefore, ferroptosis might operate upstream of the processes of inflammation, apoptosis, and necroptosis in CIN.

We found that treatment with cisplatin augmented renal iron content, with increase in the expression of TfR and FTH proteins, indicating increased iron uptake and storage in the kidney. In addition, renal ferrous iron content also increased with cisplatin-treatment; this result seems to be contradictory to the observed trends in FTH protein expression, as the ferroxidase activity of FTH catalyzes the conversion of ferrous iron to ferric iron, and ferric iron is stored in ferritin [23]. A recent study showed that cisplatin binds to FTH without affecting its iron binding capability but affects its catalytic activity [24]. Moreover, iron reduction by DFO prevented cisplatin-induced increase in COX-2 expression and lipid peroxidation in the kidney. Therefore, cisplatin-induced increases in ferrous iron levels may be due to the reduced catalytic activity of FTH, contributing to

the induction of ferroptosis through iron-mediated lipid peroxidation via the Fenton reaction.

GPX4 plays an important role in protecting cells from ferroptosis by maintaining redox homeostasis [5]. Dysfunction of GPX4 induces ferroptosis by inducing the formation lipid hydroperoxides via ferrous-dependent formation of toxic lipid reactive oxygen species (ROS). Two recent studies have shown that cisplatin induces ferroptosis in the kidneys [25,26]. Cisplatin treatment reduced GPX4 protein [26] and GSH-peroxidase activity [27]. However, in our model, renal GPX4 protein levels did not change despite cisplatin treatment, although kidney GPX4 mRNA levels reduced. Therefore, cisplatin-induced ferroptosis is mainly caused by lipid peroxidation, and the involvement of GPX4 in CIN is unclear.

Ferroptosis is emerging as a new target in cancer therapeutics and has recently been shown to be a mechanism of active cancer cell death induced by classic chemotherapeutic agents. Cisplatin triggers ferroptosis by inhibiting GPX4, resulting in GSH depletion in A549 and HCT116 cells [28]. Cisplatin equally induces ferroptosis through intracellular free iron-induced induced ferritinophagy in lung cancer cells [29]. Thus, cisplatin exerts its anti-cancer effects through DNA damage and inhibition of DNA

synthesis, as well as through the induction ferroptosis [30]. Moreover, the anti-cancer effects of cisplatin are further enhanced through synergistic action with ferroptosis inducers such as erastin or RSL3 [28,29]. In addition, ferroptosis plays a detrimental role in the pathogenesis of kidney injury, as its inhibition was found to prevent kidney injury induced by ischemia/reperfusion [31], folic acid [22], and oxalate crystals [11]. In this study, we demonstrated that CIN is suppressed by ferroptosis inhibitors and iron chelators, indicating that the effects of ferroptosis induced by cisplatin in kidney cells are different from those in cancer cells.

In the present study, we used DFO to examine the effect of an iron chelator on cisplatin-induced renal ferroptosis in mice. DFO must be administered subcutaneously or intravenously, while other iron chelator such as deferiprone (DFP) or deferasirox (DFX) is orally bioavailable drug. In addition, DFP and DFX have a few affinities for other metals including copper and zinc compared to DFO [32], which might contribute to specific iron chelation without affecting other metals in the body. DFP or DFX is thought to be favorable for the prevention of CIN in clinical practice.

In conclusion, ferroptosis may play a role in the pathophysiology of CIN by increasing both total iron and ferrous iron content. Further investigation is necessary to confirm ferroptosis as a preventive target against CIN.

Study Approval

All experimental procedures involving mice were performed in accordance with the guidelines of the Animal Research Committee of the Tokushima University Graduate School, and the protocol was approved by the Institutional Review Board of Tokushima University Graduate School for animal protection (Permit Number: T30-74).

Author contributions: Yasumasa Ikeda: Conceptualization, Methodology, Validation, Investigation, Writing-Original draft preparation, Supervision. **Hirofumi Hamano:**

Investigation, Writing- Reviewing and Editing. **Yuya Horinouchi:** Writing- Reviewing and Editing. **Licht Miyamoto:** Writing- Reviewing and Editing. **Tasuku Hirayama:** Resources and Writing- Reviewing and Editing. **Hideko Nagasawa:** Resources and Writing- Reviewing and Editing. **Toshiaki Tamaki:** Writing- Reviewing and Editing. **Koichiro Tsuchiya:** Writing- Reviewing and Editing.

Declarations of interest: None:

References

1. Campbell AB, Kalman SM, Jacobs C. Plasma platinum levels: relationship to cisplatin dose and nephrotoxicity. Cancer Treat Rep 1983;67(2):169-172.
2. Ciarimboli G, Ludwig T, Lang D, Pavenstadt H, Koepsell H, Piechota HJ, Haier J, Jaehde U, Zisowsky J, Schlatter E. Cisplatin nephrotoxicity is critically mediated via the human organic cation transporter 2. Am J Pathol 2005;167(6):1477-1484.
3. Ozkok A, Edelstein CL. Pathophysiology of cisplatin-induced acute kidney injury. Biomed Res Int 2014;2014:967826.
4. Santoso JT, Lucci JA, 3rd, Coleman RL, Schafer I, Hannigan EV. Saline, mannitol, and furosemide hydration in acute cisplatin nephrotoxicity: a randomized trial. Cancer Chemother Pharmacol 2003;52(1):13-18.
5. Dixon SJ, Lemberg KM, Lamprecht MR, Skouta R, Zaitsev EM, Gleason CE, Patel DN, Bauer AJ, Cantley AM, Yang WS, Morrison B, 3rd, Stockwell BR. Ferroptosis: an iron-dependent form of nonapoptotic cell death. Cell 2012;149(5):1060-1072.
6. Li J, Cao F, Yin HL, Huang ZJ, Lin ZT, Mao N, Sun B, Wang G. Ferroptosis: past, present and future. Cell Death Dis 2020;11(2):88.

7.   Mou Y, Wang J, Wu J, He D, Zhang C, Duan C, Li B. Ferroptosis, a new form of cell death: opportunities and challenges in cancer. J Hematol Oncol 2019;12(1):34.

8.   Skouta R, Dixon SJ, Wang J, Dunn DE, Orman M, Shimada K, Rosenberg PA, Lo DC, Weinberg JM, Linkermann A, Stockwell BR. Ferrostatins inhibit oxidative lipid damage and cell death in diverse disease models. J Am Chem Soc 2014;136(12):4551-4556.

9.   Li Q, Han X, Lan X, Gao Y, Wan J, Durham F, Cheng T, Yang J, Wang Z, Jiang C, Ying M, Koehler RC, Stockwell BR, Wang J. Inhibition of neuronal ferroptosis protects hemorrhagic brain. JCI Insight 2017;2(7):e90777.

10.   Fang X, Wang H, Han D, Xie E, Yang X, Wei J, Gu S, Gao F, Zhu N, Yin X, Cheng Q, Zhang P, Dai W, Chen J, Yang F, Yang HT, Linkermann A, Gu W, Min J, Wang F. Ferroptosis as a target for protection against cardiomyopathy. Proc Natl Acad Sci U S A 2019;116(7):2672-2680.

11.   Linkermann A, Skouta R, Himmerkus N, Mulay SR, Dewitz C, De Zen F, Prokai A, Zuchtriegel G, Krombach F, Welz PS, Weinlich R, Vanden Berghe T, Vandenabeele P, Pasparakis M, Bleich M, Weinberg JM, Reichel CA, Brasen JH, Kunzendorf U, Anders HJ, Stockwell BR, Green DR, Krautwald S. Synchronized renal tubular cell death involves ferroptosis. Proc Natl Acad Sci U S A 2014;111(47):16836-16841.

12.   Baliga R, Zhang Z, Baliga M, Ueda N, Shah SV. In vitro and in vivo evidence suggesting a role for iron in cisplatin-induced nephrotoxicity. Kidney Int 1998;53(2):394-401.

13.   Hamano H, Ikeda Y, Goda M, Fukushima K, Kishi S, Chuma M, Yamashita M, Niimura T, Takechi K, Imanishi M, Zamami Y, Horinouchi Y, Izawa-Ishizawa Y, Miyamoto L, Ishizawa K, Fujino H, Tamaki T, Aihara KI, Tsuchiya K. Diphenhydramine may be a preventive medicine against cisplatin-induced kidney toxicity. Kidney Int 2020.

14.   Tajima S, Ikeda Y, Sawada K, Yamano N, Horinouchi Y, Kihira Y, Ishizawa K, Izawa-Ishizawa Y, Kawazoe K, Tomita S, Minakuchi K, Tsuchiya K, Tamaki T. Iron reduction by deferoxamine leads to amelioration of adiposity via the regulation of oxidative stress and inflammation in obese and type 2 diabetes KKAy mice. Am J Physiol Endocrinol Metab 2012;302(1):E77-86.

15. Hirayama T, Niwa M, Hirosawa S, Nagasawa H. High-Throughput Screening for the Discovery of Iron Homeostasis Modulators Using an Extremely Sensitive Fluorescent Probe. ACS Sens 2020;5(9):2950-2958.

16. Ikeda Y, Satoh A, Horinouchi Y, Hamano H, Watanabe H, Imao M, Imanishi M, Zamami Y, Takechi K, Izawa-Ishizawa Y, Miyamoto L, Hirayama T, Nagasawa H, Ishizawa K, Aihara KI, Tsuchiya K, Tamaki T. Iron accumulation causes impaired myogenesis correlated with MAPK signaling pathway inhibition by oxidative stress. FASEB J 2019;33(8):9551-9564.

17. Ikeda Y, Horinouchi Y, Hamano H, Hirayama T, Kishi S, Izawa-Ishizawa Y, Imanishi M, Zamami Y, Takechi K, Miyamoto L, Ishizawa K, Aihara KI, Nagasawa H, Tsuchiya K, Tamaki T. Dietary iron restriction alleviates renal tubulointerstitial injury induced by protein overload in mice. Sci Rep 2017;7(1):10621.

18. Yang WS, SriRamaratnam R, Welsch ME, Shimada K, Skouta R, Viswanathan VS, Cheah JH, Clemons PA, Shamji AF, Clish CB, Brown LM, Girotti AW, Cornish VW, Schreiber SL, Stockwell BR. Regulation of ferroptotic cancer cell death by GPX4. Cell 2014;156(1-2):317-331.

19. Pabla N, Dong Z. Cisplatin nephrotoxicity: mechanisms and renoprotective strategies. Kidney Int 2008;73(9):994-1007.

20. Miller RP, Tadagavadi RK, Ramesh G, Reeves WB. Mechanisms of Cisplatin nephrotoxicity. Toxins (Basel) 2010;2(11):2490-2518.

21. Xu Y, Ma H, Shao J, Wu J, Zhou L, Zhang Z, Wang Y, Huang Z, Ren J, Liu S, Chen X, Han J. A Role for Tubular Necroptosis in Cisplatin-Induced AKI. J Am Soc Nephrol 2015;26(11):2647-2658.

22. Martin-Sanchez D, Ruiz-Andres O, Poveda J, Carrasco S, Cannata-Ortiz P, Sanchez-Nino MD, Ruiz Ortega M, Egido J, Linkermann A, Ortiz A, Sanz AB. Ferroptosis, but Not Necroptosis, Is Important in Nephrotoxic Folic Acid-Induced AKI. J Am Soc Nephrol 2017;28(1):218-229.

23. Theil EC. Ferritin: structure, gene regulation, and cellular function in animals, plants, and microorganisms. Annu Rev Biochem 1987;56:289-315.

24. Annunziata A, Amoresano A, Cucciolito ME, Esposito R, Ferraro G, Iacobucci I, Imbimbo P, Lucignano R, Melchiorre M, Monti M, Scognamiglio C, Tuzi A, Monti DM, Merlino A, Ruffo F. Pt(II) versus Pt(IV) in Carbene Glycoconjugate

Antitumor Agents: Minimal Structural Variations and Great Performance Changes. Inorg Chem 2020;59(6):4002-4014.

25. Mishima E, Sato E, Ito J, Yamada KI, Suzuki C, Oikawa Y, Matsuhashi T, Kikuchi K, Toyohara T, Suzuki T, Ito S, Nakagawa K, Abe T. Drugs Repurposed as Antiferroptosis Agents Suppress Organ Damage, Including AKI, by Functioning as Lipid Peroxyl Radical Scavengers. J Am Soc Nephrol 2020;31(2):280-296.

26. Hu Z, Zhang H, Yi B, Yang S, Liu J, Hu J, Wang J, Cao K, Zhang W. VDR activation attenuate cisplatin induced AKI by inhibiting ferroptosis. Cell Death Dis 2020;11(1):73.

27. Ognjanovic BI, Djordjevic NZ, Matic MM, Obradovic JM, Mladenovic JM, Stajn AS, Saicic ZS. Lipid peroxidative damage on Cisplatin exposure and alterations in antioxidant defense system in rat kidneys: a possible protective effect of selenium. Int J Mol Sci 2012;13(2):1790-1803.

28. Guo J, Xu B, Han Q, Zhou H, Xia Y, Gong C, Dai X, Li Z, Wu G. Ferroptosis: A Novel Anti-tumor Action for Cisplatin. Cancer Res Treat 2018;50(2):445-460.

29. Zhang X, Sui S, Wang L, Li H, Zhang L, Xu S, Zheng X. Inhibition of tumor propellant glutathione peroxidase 4 induces ferroptosis in cancer cells and enhances anticancer effect of cisplatin. J Cell Physiol 2020;235(4):3425-3437.

30. Basu A, Krishnamurthy S. Cellular responses to Cisplatin-induced DNA damage. J Nucleic Acids 2010;2010.

31. Friedmann Angeli JP, Schneider M, Proneth B, Tyurina YY, Tyurin VA, Hammond VJ, Herbach N, Aichler M, Walch A, Eggenhofer E, Basavarajappa D, Radmark O, Kobayashi S, Seibt T, Beck H, Neff F, Esposito I, Wanke R, Forster H, Yefremova O, Heinrichmeyer M, Bornkamm GW, Geissler EK, Thomas SB, Stockwell BR, O'Donnell VB, Kagan VE, Schick JA, Conrad M. Inactivation of the ferroptosis regulator Gpx4 triggers acute renal failure in mice. Nat Cell Biol 2014;16(12):1180-1191.

32. Crisponi G, Nurchi VM, Crespo-Alonso M, Sanna G, Zoroddu MA, Alberti G, Biesuz R. A Speciation Study on the Perturbing Effects of Iron Chelators on the Homeostasis of Essential Metal Ions. PLoS One 2015;10(7):e0133050.

Figure legends

Figure 1: Effects of cisplatin on hydroxy radical and ferrous iron levels in the kidney.
(A) Representative staining of kidney sections from the control and cisplatin-injected
mice with FerroOrange, hydroxyphenyl fluorescein (HPF), and 4',6-diamidino-2-
phenylindole (DAPI). (B) Semi-quantitative analysis of HPF fluorescence intensities.
Values are expressed as mean ± SEM, *P < 0.05, n = 7–8 in each group. (C) Semi-
quantitative analysis of RhoNox-4 fluorescence intensities. Values are expressed as mean
± SEM, *P < 0.05, n = 7–8 in each group. (D) Renal iron levels in mice treated with or
without cisplatin. Values are expressed as mean ± SEM, *P < 0.05, n = 7–8 in each group.
TfR (E) and FTH (F) levels in mice treated with or without cisplatin. Representative
protein bands and semi-quantitative analysis of TfR and FTH levels in the kidneys of
mice in each group. Values are expressed as mean ± SEM, *P < 0.05, **P < 0.01, n = 6–
9 in each group.

Figure 2: Effects of cisplatin on ferroptosis. (A) Left panel: COX-2 and β-actin mRNA
levels in the kidneys of mice in each group. Values are expressed as mean ± SEM, *P <
0.05, n = 8 in each group. Right panel: Representative protein bands and semi-quantitative

analysis of COX-2 expression in the kidneys of mice in each group. Values are expressed as mean ± SEM, *P < 0.05, n = 6 in each group. (B) Left panel: GPX-4 mRNA expression levels in the kidneys of mice in each group. Values are expressed as mean ± SEM, *P < 0.05, n = 8 in each group. Right panel: Representative protein bands and semi-quantitative analysis of GPX-4 and β-actin expression in the kidneys of mice in each group. Values are expressed as mean ± SEM, *P < 0.05, n = 6 in each group. (C) Left panel: Representative protein bands of 4-hydroxynonenal (HNE) and β-actin in the kidneys of mice. Right panel: Semi-quantitative analysis of densitometry for 4-HNE. Values are expressed as mean ± SEM, *P < 0.05, **P < 0.01, n = 5 in each group. (D) Representative images of 4-HNE staining in the kidneys of mice in each group.

Figure 2: Ferrostatin-1 (Fer-1) inhibits cisplatin-induced nephrotoxicity in mice. (A) Left panel: Representative hematoxylin and eosin staining (HE) of the kidney sections from mice in the control group and from cisplatin-injected mice treated with vehicle or Fer-1. Right panel: Quantitative analysis of the renal tubular damage score. Values are expressed as mean ± SEM. *P < 0.05; n = 5 in each group. (B) mRNA levels of kidney injury markers (Kim-1 and lipocalin-2) in the kidneys of mice in each group. Values are

expressed as mean ± SEM. **$P < 0.01$, n = 8–9 in each group. (C) Fer-1 prevents cisplatin-induced upregulation of renal inflammation. Quantitative analysis of inflammatory cytokine mRNA expression in the kidneys of mice in each group. Values are expressed as mean ± SEM. **$P < 0.01$, n = 8–9 in each group.

Figure 4: Inhibitory effects of ferroptosis on apoptosis and necroptosis in cisplatin-induced nephrotoxicity. (A) Left panel: Representative images of TdT-mediated dUTP nick end labeling (TUNEL) staining in the kidneys of mice in each group. Right panel: Semi-quantitative analysis of TUNEL-positive cells. Values are expressed as mean ± SEM, *$P < 0.05$, n = 5 in each group. (B) Upper panel: Representative protein bands of cleaved caspase-3 (Casp-3) and β-actin in the kidneys of mice. Right panel: Semi-quantitative analysis of densitometry for cleaved Casp-3. Values are expressed as mean ± SEM, *$P < 0.05$, **$P < 0.01$, n = 8 in each group. (C) mRNA levels of necroptosis markers (RIPK3 and MLKL) in the kidneys of mice in each group. Values are expressed as mean ± SEM. *$P < 0.05$, **$P < 0.01$, n = 8 in each group.

Figure 5: Effects of deferoxamine (DFO) on cisplatin-induced nephrotoxicity via the ferroptosis pathway. (A) Representative protein bands and semi-quantitative analysis of

COX-2 and 4-HNE expression in the kidneys of mice in each group. Values are expressed as mean ± SEM, *P < 0.05, n = 6 in each group. (B) Left panel: Representative hematoxylin and eosin staining (HE) of the kidney sections of mice in the control group, cisplatin-injected mice treated with vehicle or DFO. Right panel: Quantitative analysis of the renal tubular damage score. Values are expressed as mean ± SEM. *P < 0.05; n = 8 in each group. DFO prevents cisplatin-induced renal injury (C) and inflammation (D). Quantitative analysis of mRNA levels of kidney injury markers and inflammatory cytokines and in mice in each group. Values are expressed as mean ± SEM. *P < 0.05, **P < 0.01, n = 8 in each group.
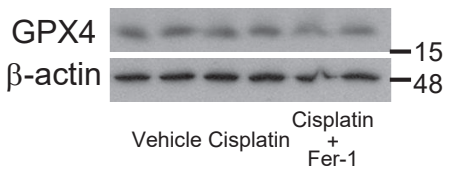
Figure 1-5

Figure1 Ikeda, et al.

(A)

(B)

(C)

(D)

(E)

(E)

Figure 2 Ikeda, et al.

(A)

COX-2

β-actin

Vehicle Cisplatin
Cisplatin
+
Fer-1

— 75

— 48

COX-2 mRNA
(Relative fold change)

35
30
25
20
15
10
5
0

** **

Vehicle Cisplatin
Cisplatin
+
Fer-1

COX-2 protein
(Relative fold change)

6
5
4
3
2
1
0

* *

Vehicle Cisplatin
Cisplatin
+
Fer-1

(B)

GPX4

β-actin

Vehicle Cisplatin
Cisplatin
+
Fer-1

— 15

— 48

GPX4 mRNA
(Relative fold change)

1.5
1
0.5
0

** **

Vehicle Cisplatin
Cisplatin
+
Fer-1

GPX4 protein
(Relative fold change)

1.5
1
0.5
0

Vehicle Cisplatin
Cisplatin
+
Fer-1

(C)

4-HNE

β-actin

Vehicle   Cisplatin   Cisplatin
+
Fer-1

— 48
— 35
— 25
— 20

— 48

4-HNE protein
(Relative fold change)

2.5
2
1.5
1
0.5

* *

Vehicle Cisplatin
Cisplatin
+
Fer-1

(D)

Vehicle   Cisplatin   Cisplatin
+
Fer-1

100μm

Figure 3 Ikeda, et al.
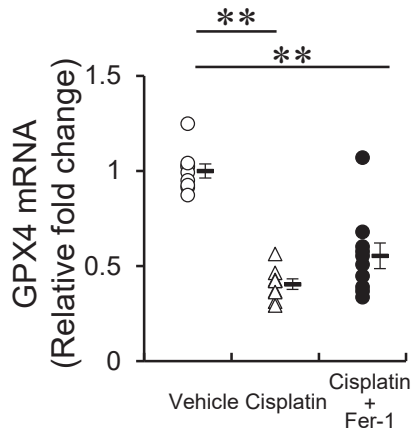
(A)

Vehicle   Cisplatin   Cisplatin+Fer1

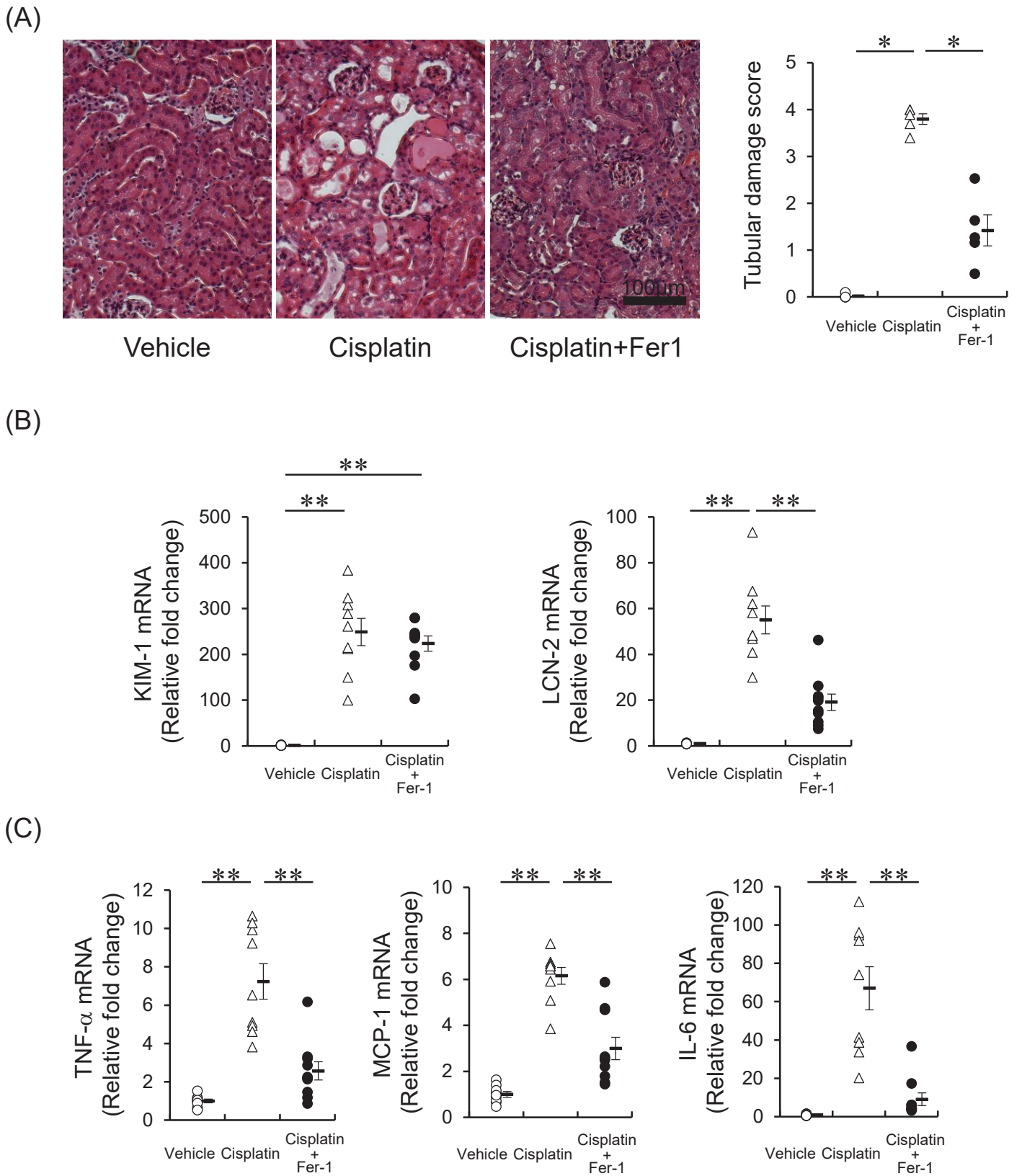(B)

(C)

Figure 4 Ikeda, et al.

(A)

(B)

(C)

Figure 5 Ikeda, et al.

(A)

(B)

(C)

(D)

Table 1. Sets of primer sequences

	Forward	Reverse
Mouse cyclooxygenase (COX)-2	TGCAGAATTGAAAGCCCTCT	CCCCAAAGATAGCATCTGGA
Mouse glutathione peroxidase (GPX)-4	CTCCATGCACGAATTCTCAG	GCACACGAAACCCCTGTACT
Mouse kidney injury molecule (KIM)-1	AAACCAGAGATTCCCACACG	GTCGTGGGTCTTCCTGTAGC
Mouse lipocalin (LCN)-2	TGGAAGAACCAAGGAGCTGT	GGTGGGGACAGAGAAGATGA
Mouse tumor necrosis factor (TNF)-α	ACGGCATGGATCTCAAAGAC	GTGGGTGAGGAGCACGTAGT
Mouse monocyte chemoattractant protein (MCP)-1	GGAGCTCATGATGTGAGCAA	GACCAGGCAAGGGAATTACA
Mouse interleuikin-6 (IL-6)	CCGGAGAGGAGACTTCACAG	TCCACGATTTCCCAGAGAAC
Mouse receptor-interacting kinase (RIPK)3	GGGACCTCAAGCCCTCTAAT	GATCCTGATCCTGACCCTGA
Mouse mixed lineage kinase domain-like (MLKL)	GAGTTGTTGCGGCAAATCAT	CACCTTCTTGTCCGTGGATT
36B4	GCTCCAAGCAGATGCAGCA	CCGGATGTGAGGCAGCAG

Table 2. Body weight, kidney weight, and renal function in vehicle-treated mice and cisplatin-treated mice with or without Ferrostain-1

	Vehicle	Cisplatin	Cisplatin+Ferrostatin-1
Initial body weight (g)	22.4 ± 0.4	23.1 ± 0.4	23.0 ± 0.2
Post body weight (g)	23.5 ± 0.4	19.8 ± 0.4**	20.1 ± 0.3**
Right kidney weight (mg)	134.6 ± 3.0	129.0 ± 3.0	128.5 ± 3.6
Left kidney weight (mg)	128.1 ± 3.9	121.4 ± 3.6	117.3 ± 3.9
BUN (mg/dl)	24.6 ± 1.46	69.9 ± 6.2**	32.5 ± 1.7**##
Creatinine (mg/dl)	0.11 ± 0.00	0.42 ± 0.03**	0.16 ± 0.01**##

Data represent mean ± SEM; n = 10; **$P < 0.01$ vs. vehicle mice, ##$P < 0.01$ vs. cisplatin mice.

Table 3. Body weight, kidney weight, and renal function in vehicle-treated mice and cisplatin-treated mice with or without Deferoxamine

	Vehicle	Cisplatin	Cisplatin+Deferoxamine
Initial body weight (g)	24.0 ± 0.6	24.6 ± 0.5	24.9 ± 0.4
Post body weight (g)	24.6 ± 0.5	21.6 ± 0.6**	22.4 ± 0.3*
Right kidney weight (mg)	140.0 ± 4.8	135.3 ± 4.9	132.4 ± 5.5
Left kidney weight (mg)	136.0 ± 3.9	133.4 ± 3.5	133.4 ± 3.9
BUN (mg/dl)	24.7 ± 1.1	70.4 ± 7.8**	32.5 ± 2.1[##]
Creatinine (mg/dl)	0.11 ± 0.01	0.42 ± 0.04**	0.26 ± 0.02**[##]

Data represent mean $\pm$ SEM; $n = 8$; *$P < 0.05$, **$P < 0.01$ vs. vehicle mice, [#]$P < 0.05$, [##]$P < 0.01$ vs. cisplatin mice.